

Anisotropy of spin splitting and spin relaxation in lateral quantum dots

Vladimir I. Fal'ko^{1,2}, B.L. Altshuler^{2,3}, O. Tsypliyatev¹

¹ *Physics Department, Lancaster University, Lancaster LA1 4YB, United Kingdom*

² *Physics Department, Princeton University, Princeton, NJ 08540 and*

³ *NEC-Labs America, Inc., 4 Independence Way, Princeton, NJ 08540*

(Dated: March 23, 2022)

Inelastic spin relaxation and spin splitting ε_s in lateral quantum dots are studied in the regime of strong in-plane magnetic field. Due to both g-factor energy dependence and spin-orbit coupling ε_s demonstrates a substantial non-linear magnetic field dependence similar to that observed by R.Hanson *et al* [Phys. Rev. Lett. **91**, 196802 (2003)]. It also varies with the in-plane orientation of magnetic field due to crystalline anisotropy of spin-orbit coupling. Spin relaxation rate is also anisotropic, the anisotropy increasing with the field. When the magnetic length is less than the 'thickness' of GaAs dot, the relaxation can be order of magnitude faster for $\mathbf{B} \parallel [100]$ than for $\mathbf{B} \parallel [110]$.

Proposals to use electronic spin in quantum dots for quantum information processing have fuelled extensive studies of spin-orbit (SO) coupling in heterostructures as means to manipulate the electron spin¹ and as a source of spin relaxation. Recent theories^{2,3,4} and experiments^{5,6,7} suggest that spin relaxation in quantum dots is strongly suppressed by electron confinement but may be sped-up by a magnetic field, in particular, by the field parallel to the plane of the lateral structure.

It is customary to assume that an in-plane magnetic field couples only to spin of the electron. In this approximation one can describe spin relaxation in terms of effective two-dimensional (2D) SO coupling^{2,3,4}. This approach can be justified provided that $\lambda_B > \lambda_z$, where $\lambda_B = \sqrt{\hbar/eB}$ is magnetic length and λ_z is the extent of the subband wave function across the 2D plane. In the opposite limit that corresponds to a strong magnetic field, $\lambda_B \ll \lambda_z$, subbands in a heterostructure transform into bulk Landau levels (magneto-subbands) thus changing parameters of the effective 2D motion⁸. This effect has been observed in optical and FIR spectroscopy of low-density GaAs/AlGaAs heterostructures⁹, resonant tunnelling in double-barrier devices¹⁰, and in quantum transport characteristics of lateral dots¹¹.

In this Letter, we propose a theory of the spin relaxation of electrons in lateral dots in a strong in-plane magnetic field. The field effect on the orbital electron motion transforms states in low-density heterostructures into magneto-subbands. We take into account this crossover as well as the Dresselhaus-type spin-orbit coupling in GaAs¹². We show that at high fields both the inelastic spin-flip time T_1 at low temperatures $kT \ll \varepsilon_s$ and the electron spin splitting ε_s depend on the magnetic field orientation with respect to crystallographic axes, which can be used to distinguish the SO coupling-induced effects from those caused by a hyperfine interaction with nuclei. We also present analytical description of ε_s and T_1 dependences on both the magnitude and direction of the magnetic field.

The Hamiltonian of electrons in a dot made of a lateral GaAs/AlGaAs structure grown in direction $\mathbf{l}_z = [001]$

can be written as

$$\hat{H}_{3D} = \frac{\hat{p}_z^2 + \hat{p}_X^2 + \hat{p}_Y^2}{2m} + V(\mathbf{r}) + \frac{g\mu_B}{2}\sigma_X + \hat{H}_{so},$$

$$\hat{H}_{so} = \gamma\hbar^{-3} \sum_{kij=x,y,z} \epsilon^{ijk} \hat{p}_i \hat{p}_j \sigma_j \hat{p}_i. \quad (1)$$

In Eq. (1) we use two systems of in-plane coordinates. Axes x and y (used in the SO coupling term \hat{H}_{so}) are determined by crystallographic directions $[100]$ and $[010]$, respectively. Axis X is directed along the in-plane field $\mathbf{B} = \mathbf{l}_X B$, with $\mathbf{l}_X = (l_x, l_y, 0)$ and Y along $\mathbf{l}_Y = (-l_y, l_x, 0)$. In Eq. (1) the kinematic, $p_\alpha \equiv -i\hbar\partial_\alpha$ and canonical, \hat{p}_α momenta are written in the coordinate system X and Y . We use the Landau gauge $\mathbf{A} = -(z-a)B\mathbf{l}_Y$, so that $\hat{p}_z = p_z$, $\hat{p}_X = p_X$ and $\hat{p}_Y = p_Y - \frac{e}{c}B(z-a)$, with a to be specified later.

In the spin part of \hat{H}_{3D} , μ is Bohr magneton, g-factor in GaAs¹³ is $g \approx -0.44 + \hat{\mathbf{p}}^2 g'$, ϵ^{ijk} is the antisymmetric tensor, and SO coupling constant γ according to Refs.^{14,15,16} is $\gamma = (26 \pm 6) \text{ eV \AA}^3$. \hat{H}_{so} in Eq. (1) is written in the form which guarantees that it is Hermitian, despite the non-commutativity of operators \hat{p}_x and \hat{p}_y with \hat{p}_z ¹⁷.

The dot is formed by a potential profile $V = V_z(z) + \frac{1}{2}m\vartheta^2(X^2 + Y^2)$, which is stronger in the heterostructure growth direction \mathbf{l}_z than within the XY plane. We consider two particular cases: triangular well $V_z = Fz$ and parabolic well $V_z(z) = \frac{1}{2}m\omega_z^2 z^2$. The wave functions $|n, p_X, p_Y\rangle$ of electrons in the n -th magneto-subband and their 2D dispersion, $\varepsilon_n(p_Y) + \frac{1}{2m}p_X^2$ is determined by

$$\hat{H}_z = \frac{1}{2m}\hat{p}_z^2 + V_z(z) + \frac{1}{2}m\omega_c^2 [z - a - \lambda_B^2 p_Y]^2, \quad (2)$$

whereas the parameter a is chosen in such a way that the lowest subband dispersion $\varepsilon_0(p_Y)$ has minimum at $p_Y = 0$. This defines $\tilde{z} = z - a$ and $m_Y^{-1} = \partial_{p_Y}^2 \varepsilon_0(p_Y)|_{p_Y=0}$. For a triangular well, we describe magneto-subbands using the function of a parabolic cylinder¹⁸ and evaluate a and $m_Y \equiv \eta m$ numerically. For a parabolic well, harmonic oscillator functions give $a = 0$ and $\eta = 1 + \omega_c^2/\omega^2$.

Since electron confinement across the plane is much stronger than in lateral directions, $p_X, p_Y \ll p_z$, we substitute $\hat{p}_Y = p_Y - \frac{e}{c}B\tilde{z} = p_Y - m\omega_c\tilde{z}$, $\hat{p}_x =$

$l_x p_X - l_y p_Y + l_y m \omega_c \tilde{z}$ and $\hat{p}_y = l_y p_X + l_x p_Y - l_x m \omega_c \tilde{z}$ into \hat{H}_{3D} , expand it in powers of kinematic momenta p_X and p_Y (up to quadratic terms) and derive the effective 2D Hamiltonian $\hat{H}_{2D}(p_X, p_Y, \tilde{\sigma})$. In particular, when analysing SO coupling, we expand \hat{H}_{so} up to linear order in p_Y and p_X ,

$$\begin{aligned} \hat{H}_{so} &\approx \hat{H}_{so}^0 + \hat{H}_{so}^1, \text{ where} \\ \frac{\hat{H}_{so}^0}{\gamma} &= l_x l_y \left[2 \frac{\hat{p}_z \tilde{z} \hat{p}_z}{\hbar^2 \lambda_B^2} - \frac{\tilde{z}^3}{\lambda_B^6} \right] \sigma_X \\ &\quad + (l_x^2 - l_y^2) \frac{\hat{p}_z \tilde{z} \hat{p}_z}{\hbar^2 \lambda_B^2} \sigma_Y + (l_x^2 - l_y^2) \left(\frac{\tilde{z} \hat{p}_z \tilde{z}}{\hbar \lambda_B^4} \right) \sigma_z, \\ \frac{\hat{H}_{so}^1}{\gamma} &= (l_x^2 - l_y^2) \left[\left(\frac{\hat{p}_z^2}{\hbar^2} - \frac{\tilde{z}^2}{\lambda_B^4} \right) \frac{p_X \sigma_X}{\hbar} - \frac{\hat{p}_z^2}{\hbar^2} \frac{p_Y \sigma_Y}{\hbar} \right] \\ &\quad - l_x l_y \left(\frac{2 \hat{p}_z^2}{\hbar^2} + \frac{\tilde{z}^2}{\lambda_B^4} \right) \frac{p_X \sigma_Y}{\hbar} \\ &\quad - l_x l_y \left(\frac{2 \hat{p}_z^2}{\hbar^2} - \frac{3 \tilde{z}^2}{\lambda_B^4} \right) \frac{p_Y \sigma_X}{\hbar} \\ &\quad - ([l_x^2 - l_y^2] p_Y + 2 l_x l_y p_X) \frac{\tilde{z} \hat{p}_z + \hat{p}_z \tilde{z}}{\hbar^2 \lambda_B^2} \sigma_z. \end{aligned} \quad (3)$$

In both \hat{H}_{so}^0 and \hat{H}_{so}^1 the last term does not contribute to the effective 2D Hamiltonian: for magneto-subbands determined by \hat{H}_z in Eq. (2) $\langle 0, p_X, p_Y | \tilde{z} p_z \tilde{z} | 0, p_X, p_Y \rangle = 0$ and $\langle 0, p_X, p_Y | \tilde{z} p_z + p_z \tilde{z} | 0, p_X, p_Y \rangle = 0$.

The first term in \hat{H}_{so}^0 yields an anisotropic addition to the 2D electron spin splitting linear in γ . The second term slightly turns the spin quantization axis off the magnetic field $\mathbf{B} = \mathbf{l}_X B$. It can be neglected as long as we restrict ourselves by the lowest order in γ . Thus,

$$\begin{aligned} \varepsilon_s &= g \mu B - l_x l_y \gamma \lambda_z^{-3} A_s, \\ g &\approx -0.44 + \langle 0 | p_z^2 | 0 \rangle g', \quad \lambda_z = (\hbar^2 / m F)^{1/3}, \\ A_s &= \frac{\lambda_z^3 \langle 0 | \tilde{z}^3 | 0 \rangle}{\lambda_B^6} - 2 \frac{\lambda_z^3 \langle 0 | p_z \tilde{z} p_z | 0 \rangle}{\lambda_B^2 \hbar^2}. \end{aligned} \quad (4)$$

The anisotropy of spin splitting is crucially sensitive to the inversion asymmetry of the confinement potential V_z , thus it is a peculiarity of heterostructures. The anisotropy effect in Eq.(4) is maximal in a field oriented along crystallographic directions $[110]$ or $[1\bar{1}0]$. The field dependence of the anisotropic part of spin splitting is characterised by the parameter A_s . In a weak magnetic field, $\omega_c \hbar < \varepsilon_1 - \varepsilon_0$, perturbation theory analysis gives $A_s \approx 2.46 \frac{m \lambda_z^2}{\hbar} \omega_c = 3.42 \omega_c \hbar / (\varepsilon_1 - \varepsilon_0)$ leading to the anisotropy of linear g-factor. The field dependence $A_s(B)$ at high fields is shown in Fig.1(a). For GaAs/AlGaAs heterostructure with $\lambda_z \sim 100 \text{\AA}$ and $\gamma \sim (26 \pm 6) \text{eV \AA}^3$, Eq.(4) predicts that the spin splitting ε_s is modulated by about 10% for different orientations of the magnetic field. ε_s also includes an isotropic non-linear B -dependent part due to the g-factor dependence on the electron momentum, $\langle 0 | p_z^2 | 0 \rangle \sim B e \hbar / 2c$,

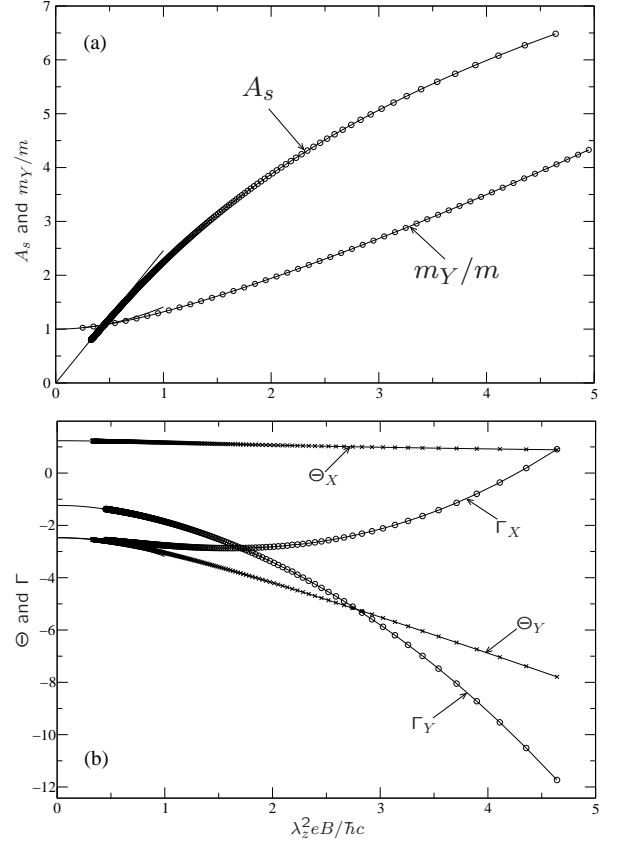


FIG. 1: Magnetic field dependence of parameters (a) A_s , $\eta = m_Y/m$ and (b) $\Theta_{X,Y}$, $\Gamma_{X,Y}$ for potential well $V_z = Fz$.

thus $g \mu B \approx -0.44 \mu B + \frac{e \hbar}{2c} g' \mu B^2$. A non-linear $\varepsilon_s(B)$ -dependence similar to that described by Eq. (4) was reported in Ref.⁵ where measurements have been made in a field applied along $[110]$ axis²¹.

In the effective 2D Hamiltonian,

$$\begin{aligned} \hat{H}_{2D} &= \frac{(p_X - \hat{a}_X)^2}{2m} + \frac{(p_Y - \hat{a}_Y)^2}{2\eta m} \\ &\quad + \frac{m v^2 (X^2 + Y^2)}{2} + \frac{\varepsilon_s}{2} \sigma_X, \\ \hat{a}_X &= -\hbar \lambda_{so}^{-1} ([l_x^2 - l_y^2] \Theta_X \sigma_X + l_x l_y \Theta_Y \sigma_Y), \\ \hat{a}_Y &= -\hbar \lambda_{so}^{-1} (l_x l_y \Gamma_X \sigma_X + [l_x^2 - l_y^2] \Gamma_Y \sigma_Y), \end{aligned} \quad (5)$$

SO coupling arises from the first three terms in \hat{H}_{so}^1 . It manifests itself via non-Abelian gauge fields \hat{a}_X, \hat{a}_Y which display an anisotropy linked both to the direction of external magnetic high field $\mathbf{B} = \mathbf{l}_X B$ and crystalline axes,

$$\begin{aligned} \Theta_X &= \hbar \lambda_z^2 (\kappa - \xi), \quad \Theta_Y = -\hbar \lambda_z^2 (2\kappa + \xi), \\ \Gamma_X &= -\hbar \lambda_z^2 (2\kappa - 3\xi) \eta, \quad \Gamma_Y = -\hbar \lambda_z^2 \kappa \eta, \\ \lambda_{so}^{-1} &= \frac{\gamma m}{\hbar^2 \lambda_z^2}, \quad \kappa = \langle 0 | \frac{p_z^2}{\hbar^3} | 0 \rangle \text{ and } \xi = \frac{\langle 0 | \tilde{z}^2 | 0 \rangle}{\hbar \lambda_B^4}. \end{aligned}$$

Fig. 1(b) shows how Θ and Γ depend on the magnetic field¹⁸ for a triangular well $V_z = Fz$ [with $\lambda_z =$

$(\hbar^2/mF)^{1/3}]$. At high fields these dependences are similar to what we found for a parabolic well $V_z(z) = \frac{1}{2}m\omega^2 z^2$ with $\lambda_z = \sqrt{2\hbar/m\omega}$,

$$\Theta_X = \frac{1}{\varrho}; \Theta_Y = \frac{1}{\varrho} - 3\varrho; \Gamma_X = \varrho^3 - 3\varrho; \Gamma_Y = -\varrho^3$$

where $\varrho = \sqrt{1 + \omega_c^2/\omega^2} \approx \lambda_z^2 eB/2\hbar c$ at $\omega_c \gg \omega$. This similarity implies that at high field we can approximate Θ, Γ , and m_Y in heterostructures by their values obtained for a parabolic well with the same λ_z .

Lateral orbital states described by \hat{H}_{2D} have the spectrum $E_{MM'} = (M + \frac{1}{2})\hbar\vartheta + (M' + \frac{1}{2})\hbar\eta\eta^{-1/2}$. The lowest level wave function¹⁸ is $|\mathbf{0}\rangle = (\pi\lambda\lambda_Y)^{-1/2} e^{-X^2/\lambda^2} e^{-Y^2/\lambda_Y^2} \varphi_0(z)$, where $\lambda = \sqrt{2\hbar/m\vartheta}$ and $\lambda_Y = \eta^{-1/4}\lambda$. Here, ϑ and $\eta^{-1/2}\vartheta$ are the frequencies of electron harmonic oscillations along the X and Y axes, respectively, and the dot states $|\mathbf{n}\rangle = |M, M'\rangle$ are characterized by quantum numbers M and M' .

The rate of the phonon-assisted spin flip $|\mathbf{0}, +\rangle \rightarrow |\mathbf{0}, -\rangle$ in the lowest order in both the e-ph interaction and SO coupling is

$$T_1^{-1} = \frac{2\pi}{\hbar} \int \frac{L^3 d\mathbf{q}}{(2\pi)^3} |A|^2 \delta(\varepsilon_s - \hbar s q), \quad (6)$$

$$A = \sum_{\mathbf{n} \neq \mathbf{0}} \left[\frac{\langle \mathbf{0} | W | \mathbf{n} \rangle \langle \mathbf{n} | h_{so}^Y | \mathbf{0} \rangle}{E_0 - E_{\mathbf{n}} + \varepsilon_s} + \frac{\langle \mathbf{0} | h_{so}^Y | \mathbf{n} \rangle \langle \mathbf{n} | W | \mathbf{0} \rangle}{E_0 - E_{\mathbf{n}} - \varepsilon_s} \right].$$

Here, $W(\mathbf{r}, \mathbf{q}) = w \cdot e^{i\mathbf{q}\mathbf{r}}/L^{3/2}$ is the phonon field with L^3 being the normalisation volume for phonons. We choose

$$|w|^2 = \left(\frac{\beta^2}{q_s} + \Xi^2 q_s \right), \text{ where } q_s = \frac{\varepsilon_s}{\hbar s}.$$

to take into account both piezoelectric (β) and deformation (Ξ) phonon potential.

Operators $h_{so}^\alpha(\hat{\mathbf{p}}, \mathbf{r})$ can be obtained using Eq. (5),

$$\vec{\sigma} \cdot \vec{h}_{so}(\hat{\mathbf{p}}, \mathbf{r}) = -\frac{p_X \hat{a}_X}{m} - \frac{p_Y \hat{a}_Y}{m_Y}. \quad (7)$$

As long as the orbital part of the Hamiltonian \hat{H}_{2D} remains T-invariant, the orbital eigenstates are real, and $\langle \mathbf{0} | e^{i\mathbf{q}\mathbf{r}} | \mathbf{n} \rangle = \langle \mathbf{n} | e^{i\mathbf{q}\mathbf{r}} | \mathbf{0} \rangle$. Moreover, $\langle \mathbf{n} | \vec{h}_{so} | \mathbf{0} \rangle = -\langle \mathbf{0} | \vec{h}_{so} | \mathbf{n} \rangle$ because spin operator $\vec{\sigma}$ changes sign under the $t \rightarrow -t$ transformation whereas the product $\vec{\sigma} \cdot \vec{h}_{so}$ remains the same (as a spin-orbit part of T-invariant H_{2D}). Consequently, two terms in the amplitude of the phonon-emission-assisted spin-flip process in Eq. (6) cancel² in the limit $\varepsilon_s \rightarrow 0$, and the transition amplitude reads

$$A = 2w\varepsilon_s \sum_{M, M' \geq 1} \frac{\langle \mathbf{0} | h_{so}^Y | M, M' \rangle \langle M, M' | e^{i\mathbf{q}\mathbf{r}} | \mathbf{0} \rangle}{\left(\hbar\vartheta M + M' \hbar\vartheta \sqrt{m/m_Y} \right)^2 - \varepsilon_s^2}. \quad (8)$$

Being generic for any T-invariant Hamiltonian¹⁹ such a cancellation should take place in all orders in p_X and p_Y ,

hence it is sufficient to analyse A using only the linear in momentum SO coupling in \hat{H}_{2D} .

In a parabolic dot operators p_X and p_Y couple the state $|\mathbf{0}\rangle = |0, 0\rangle$ only to states $|0, 1\rangle$, $|1, 0\rangle$, and

$$\begin{aligned} \langle 0, 0 | e^{i\mathbf{q}\mathbf{r}} | 1, 0 \rangle &= \langle 1, 0 | e^{i\mathbf{q}\mathbf{r}} | 0, 0 \rangle = \frac{i}{2} q_X \lambda \Lambda, \\ \langle 0, 0 | e^{i\mathbf{q}\mathbf{r}} | 0, 1 \rangle &= \langle 0, 1 | e^{i\mathbf{q}\mathbf{r}} | 0, 0 \rangle = \frac{i}{2} q_Y \lambda_Y \Lambda, \\ \Lambda &= \langle \mathbf{0} | e^{i\mathbf{q}\mathbf{r}} | \mathbf{0} \rangle \approx f(q_z) e^{-\frac{1}{8}[(q_X \lambda)^2 + (q_Y \lambda_Y)^2]}, \end{aligned} \quad (9)$$

where $f(q_z) = \int dz e^{iq_z z} |\varphi_0(z)|^2$. As a result,

$$A = \frac{w\varepsilon_s \Lambda \lambda^2}{\hbar\vartheta} \frac{1}{2\lambda_{so}} \left\{ \frac{l_x l_y \Theta_Y q_X}{1 - (\varepsilon_s/\hbar\vartheta)^2} + \frac{[l_x^2 - l_y^2] \Gamma_Y q_Y}{1 - (\varepsilon_s/\hbar\vartheta)^2 \eta} \right\}. \quad (10)$$

The angular distribution of the phonon emission is determined by the form-factor $\Lambda(\mathbf{q})$ in Eq.(9). Depending on the magnetic field, the emitted phonon wavelength $q_s = \varepsilon_s/\hbar s$ may fall into one of the following regimes:

$$\text{A) } q_s < \lambda^{-1}; \quad \text{B) } \lambda^{-1} < q_s < \lambda_Y^{-1}; \quad \text{C) } \lambda_Y^{-1} < q_s.$$

In regime A, the phonon wavelength exceeds all dimensions of quantum dot. As a result, $\Lambda \approx 1$ and phonons are emitted isotropically. In regime B, most of phonons are emitted perpendicularly to the magnetic field direction, since the phonon wavelength is shorter than the lateral dot size λ in the direction of external field. Accordingly, $e^{iq_z z} \approx 1$, $e^{-(q_Y \lambda/2)^2} \approx 1$, thus $f \approx 1$ and $|\Lambda|^2 \approx e^{-(q_X \lambda/2)^2}$. Finally, in the high-field regime C phonons are emitted across the heterostructure. Using the similarity between magneto-subband states¹⁸ and bulk Landau levels, we approximate $f \approx \exp[-(q_z \lambda_B/2)^2]$ and $|\Lambda|^2 \approx \exp[-(q_X \lambda/2)^2 - (q_Y \lambda_Y/2)^2 - \frac{1}{2}(q_z \lambda_B)^2]$.

The rate T_1^{-1} can be evaluated²⁰ using Eqs. (6)-(10),

$$\begin{aligned} T_1^{-1} &= \frac{\lambda_{so}^{-2} w_s^2}{4\pi \hbar^2 s} \left(\frac{\varepsilon_s \Gamma_Y}{\hbar\vartheta} \right)^2 Q \times \\ &\times \left\{ \frac{(l_x^2 - l_y^2)^2}{[1 - \eta \varepsilon_s^2 / \hbar^2 \vartheta^2]^2} + \frac{(\alpha l_x l_y)^2}{[1 - \varepsilon_s^2 / \hbar^2 \vartheta^2]^2} \right\}, \end{aligned} \quad (11)$$

where $w_s^2 = (\beta^2/q_s) + \Xi^2 q_s$, while Q and α are specific for each particular regime (A-C),

$$\begin{aligned} Q_A &= \frac{1}{12} (\lambda q_s)^4, & \alpha_A &= \Theta_Y / \Gamma_Y; \\ Q_B &= \frac{\sqrt{\pi}}{8} (\lambda q_s)^3, & \alpha_B &= 2\Theta_Y / q_s \lambda \Gamma_Y; \\ Q_C &= (\lambda / \lambda_Y)^3 e^{-\frac{1}{2}(q_s \lambda_B)^2}, & \alpha_C &= \Theta_Y \lambda_Y / \Gamma_Y \lambda. \end{aligned}$$

The factor in curly brackets in Eq.(11) determines the relaxation rate dependence on the magnetic field orientation. If the field is so weak that $\lambda_z < \lambda_B$, then $\frac{\Theta_Y}{\Gamma_Y} \approx 2$, $\lambda \approx \lambda_Y$, $\alpha = 2$, and T_1^{-1} turns out to be isotropic. The anisotropy develops when $\lambda_B \sim \lambda_z$ [i.e., $\eta > 1$,

$\lambda > \lambda_Y$ and $\Theta_Y/\Gamma_Y < 2$] and increases with the field. According to Eq. (11), at high fields where $\lambda_B \ll \lambda_z$ but $\varepsilon_s < \hbar\vartheta$ spin relaxes faster in a magnetic field oriented along [100] or [010] and slower when \mathbf{B} is parallel to [110] or $[1\bar{1}0]$, which was the field orientation²¹ in the experiment in Ref.⁵. In the field range where $\lambda_B \ll \lambda_z$ and $\varepsilon_s < \hbar\vartheta/\eta^{1/2}$, spin-flip rate for those two orientations has power-law different field dependences²², $T_1^{-1}(\mathbf{B}||[100]) \propto B^{17/2}$ and $T_1^{-1}(\mathbf{B}||[110]) \propto B^{7/2}$.

The anisotropy in T_1 is strongly enhanced in the vicinity of crossing of the level $|\mathbf{0}, +\rangle$ with $|0, 1, -\rangle$ or $|1, 0, -\rangle$, though the divergence of T_1^{-1} in Eq. (11) at $\varepsilon_s = \hbar\vartheta/\eta^{1/2}$ and $\varepsilon_s = \hbar\vartheta$ is an artifact of the lowest-order perturbation theory analysis and it is prevented by level anti-crossing due to SO coupling²³. For $\mathbf{B}||[100]$ or $\mathbf{B}||[010]$, spin relaxation is resonantly sped-up when $\varepsilon_s = \hbar\vartheta/\eta^{1/2}$. For $\mathbf{B}||[110]$ and $\mathbf{B}||[1\bar{1}0]$ the rate T_1^{-1} acquires a maximum at a higher field where $\varepsilon_s = \hbar\vartheta$. For samples used in Ref.⁵ $\hbar\vartheta \approx 1\text{meV}$, thus the crossing of $|\mathbf{0}, +\rangle$ and $|1, 0, -\rangle$ levels was beyond the experimental field range. However, for $\lambda_z \sim 10\text{nm}$ and $\hbar\vartheta \sim 1\text{meV}$ the crossing of levels $|\mathbf{0}, +\rangle$ and $|0, 1, -\rangle$ should enhance spin relaxation at B around $15 \div 20\text{T}$ if $\mathbf{B}||[100]$ or $\mathbf{B}||[010]$. The formula in Eq.(11)

is not exact when $\hbar\vartheta/\eta^{1/2} < \varepsilon_s < \hbar\vartheta\varepsilon_s$, nevertheless, in that field range the anisotropic behavior of $T_1^{-1}(\mathbf{B})$ persists, since the spin-flip for $\mathbf{B}||[100]$ or $\mathbf{B}||[010]$ is enhanced due to the opening of additional relaxation channel $|\mathbf{0}, +\rangle \rightarrow |0, 1, -\rangle$.

To conclude, we studied the effects of the spin-orbital coupling on the spin splitting ε_s and inelastic spin relaxation rate T_1^{-1} in lateral quantum dots at low temperatures $kT \ll \varepsilon_s$. We found that ε_s demonstrates a sizeable non-linearity and anisotropy in its field-dependence, Eq. (4). The anisotropy in the spin relaxation, Eq. (11) is predicted to be even stronger: if the magnetic field \mathbf{B} is high, $\lambda_B \ll \lambda_z$, the relaxation can be order of magnitude faster for $\mathbf{B}||[100]$ than for $\mathbf{B}||[110]$. The latter feature of the spin relaxation due to SO coupling can be used to distinguish it from the spin relaxation involving hyperfine interaction with nuclei.

We thank L.Kouwenhoven, D.Loss and C.Marcus for useful discussions. This work was supported by the EPSRC-Lancaster Portfolio Partnership, INTAS 03-51-6453, ARO/ARDA (DAAD19-02-1-0039) and DARPA under QuIST programme.

- ¹ H.-A. Engel *et al*, Phys. Rev. Lett. **93**, 106804 (2004); G. Burkard and D. Loss, Phys. Rev. Lett. **88**, 047903 (2002)
- ² A.Khaetskii and Y.Nazarov, Phys. Rev. B **61**, 12639 (2000); Phys. Rev. B **64**, 125316 (2001)
- ³ I.L. Aleiner and V.I. Fal'ko, Phys. Rev. Lett. **87**, 256801 (2001); J.-H. Creemers, P.W. Brouwer, and V.I. Fal'ko, Phys. Rev. B **68**, 125329 (2003)
- ⁴ V.Golovach, A.Khaetskii, D.Loss, Phys. Rev. Lett. **93**, 016601 (2004)
- ⁵ R.Hanson *et al*, Phys. Rev. Lett. **91**, 196802 (2003); J.M.Elzerman *et al*, Nature **430**, 431 (2004); J.M.Elzerman *et al*, Appl. Phys. Lett. **84**, 4617 (2004); M.Kroutvar *et al*, Nature **432**, 81 (2004)
- ⁶ T.Fujisawa *et al*, Nature **419**, 278 (2002)
- ⁷ D.M. Zumbühl *et al*, Phys. Rev. Lett. **89**, 276803 (2002)
- ⁸ In heterostructures with 2×10^{11} electrons per cm^2 , the reconstruction of the 2D electron spectrum has been observed⁹ in the field range $5 \div 7\text{T}$, whereas at the electron density 10^{10}cm^{-2} [*i.e.*, one electron in a 1000\AA -size quantum dot] magneto-subbands would already form at $B \sim 2 \div 3\text{T}$.
- ⁹ I. Kukushkin *et al*, JETP Lett. **51**, 436 (1990); B.Meurer, D.Heitmann, K.Ploog, Phys. Rev. B **48**, 11488 (1993)
- ¹⁰ C. Kutter *et al*, Phys. Rev. B **45**, 8749 (1992)
- ¹¹ D.M. Zumbühl *et al*, Phys. Rev. B **69**, 121305 (2004)
- ¹² F.Malcher, G.Lommer, U.Rössler, Phys. Rev. Lett. **60**, 729 (1988); R. Eppenga and M. Shuurmans, Phys. Rev. B **37**, 10923 (1988)
- ¹³ M.J.Snelling *et al*, Phys. Rev. B **44**, 11345 (1991); R.M.Hannak *et al*, Solid State Commun. **93**, 3132 (1995)
- ¹⁴ B.Jusserand *et al*, Phys. Rev. Lett. **69**, 848 (1992); B.Jusserand *et al*, Phys. Rev. B **51**, 4707 (1995); L.Wissinger *et al*, Phys. Rev. B **58**, 15375-15377 (1998)
- ¹⁵ J.B. Miller *et al*, Phys. Rev. Lett. **90**, 076807 (2003); W.

- Knap *et al*, Phys. Rev. B **53**, 3912-3924 (1996)
- ¹⁶ In low-density structures the Rashba coupling [Y.Bychkov and E.Rashba, JETP Lett. **39**, 78 (1984)] is insignificant^{12,14}.
- ¹⁷ $\hat{p}_x = l_x \hat{p}_X - l_y \hat{p}_Y$, $\hat{p}_y = l_y \hat{p}_X + l_x \hat{p}_Y$, $\sigma_x = l_x \sigma_X - l_y \sigma_Y$ and $\sigma_y = l_y \sigma_X + l_x \sigma_Y$.
- ¹⁸ $|n, 0, p_Y\rangle$ are functions of parabolic cylinder $Z^{-1}U(-E, \sqrt{2}[\tilde{z}\lambda_B^{-1} - p_Y\lambda_B\hbar^{-1} + \lambda_B^3\lambda_z^{-3}])$, where $E = (\epsilon/\hbar\omega_c) + \frac{1}{2}(\lambda_B/\lambda_z)^6 - (\lambda_B/\lambda_z)^3(\frac{a}{\lambda_B} + \frac{p_Y\lambda_B}{\hbar})$, $\lambda_z = (\hbar^2/mF)^{1/3}$, $(\lambda_B/\lambda_z)^3 = \lambda_B F/\hbar\omega_c$, Z^{-1} stands for normalisation, and the hard wall boundary condition are used at $\tilde{z} = -a$. The zero-field subband splitting is $\varepsilon_1 - \varepsilon_0 = 1.39\hbar^2/m\lambda_z^2$. When $\lambda_B \ll \lambda_z$, magneto-subband wave functions are close to Landau levels in the bulk, $\varphi_0 \sim \exp(-\tilde{z}^2/2\lambda_B^2)$. For $B = 0$, $\kappa \approx 1.24/\hbar\lambda_z^2$ and $\xi = 0$.
- ¹⁹ The contribution from the inter-subband part of the second term in \hat{H}_{so}^0 , Eqs. (3) is negligible, unless g-factor was engineered to be anomalously small.
- ²⁰ We take into account that $\int |\dots|^2 q_Y q_X d\mathbf{q} = 0$ and approximate $(\hbar s/2) \int (2\pi)^{-2} dq_z \delta(\hbar s q - \varepsilon_s) |\Lambda|^2 \approx \begin{cases} [1 - (q_X/q_s)^2 - (q_Y/q_s)^2]^{-1/2} & \text{(A)} \\ e^{-(q_X\lambda/2)^2} [1 - (q_Y/q_s)^2]^{-1/2} & \text{(B)} \\ e^{-(q_X\lambda/2)^2 - (q_Y\lambda_Y/2)^2 - \frac{1}{2}(q_s\lambda_B)^2} & \text{(C)} \end{cases}$
- ²¹ L.Kouwenhoven, private communication.
- ²² In GaAs $ms^2 \sim 10\mu\text{eV}$, $gm/2m_e \approx 1.5 \times 10^{-2}$ [m_e is the electron mass in vacuum], and $\frac{1}{2}(q_s\lambda_B)^2 = \frac{1}{2}(gm/2m_e)^2(\hbar\omega_c/ms^2) \ll 1$ up to the field $B \sim 50\text{T}$. The latter conclusion differs from that in Ref.⁴ predicting $T_1^{-1}(B)$ to reach maximum at $q_s \sim \lambda_z^{-1}$ (In Ref.⁴ the orbital effect of in-plane field has been neglected).
- ²³ D.Bulaev and D.Loss, cond-mat/0409614